MCB
Journals.ASM.org

Cessation of Epithelial Bmp Signaling Switches the Differentiation of Crown Epithelia to the Root Lineage in a β-Catenin-Dependent Manner

Zhenhua Yang,[a]* Bo Hai,[a] Lizheng Qin,[a] Xinyu Ti,[a]* Lei Shangguan,[a]* Yanqiu Zhao,[a]* Lindsey Wiggins,[a] Ying Liu,[b] Jian Q. Feng,[b] Julia Yu Fong Chang,[c]* Fen Wang,[c] Fei Liu[a]

Institute for Regenerative Medicine at Scott & White Hospital, Molecular and Cellular Medicine Department, College of Medicine, Texas A&M Health Science Center, Houston, Texas, USA[a]; Department of Biomedical Sciences, Baylor College of Dentistry, Dallas, Texas, USA[b]; Center for Cancer and Stem Cell Biology, Institute of Biosciences and Technology, Texas A&M Health Science Center, Houston, Texas, USA[c]

The differentiation of dental epithelia into enamel-producing ameloblasts or the root epithelial lineage compartmentalizes teeth into crowns and roots. Bmp signaling has been linked to enamel formation, but its role in root epithelial lineage differentiation is unclear. Here we show that cessation of epithelial Bmp signaling by Bmpr1a depletion during the differentiation stage switched differentiation of crown epithelia into the root lineage and led to formation of ectopic cementum-like structures. This phenotype is related to the upregulation of Wnt/β-catenin signaling and epithelial-mesenchymal transition (EMT). Although epithelial β-catenin depletion during the differentiation stage also led to variable enamel defect and precocious/ectopic formation of fragmented root epithelia in some teeth, it did not cause ectopic cementogenesis and inhibited EMT in cultured dental epithelia. Concomitant epithelial β-catenin depletion rescued EMT and ectopic cementogenesis caused by Bmpr1a depletion. These data suggested that Bmp and Wnt/β-catenin pathways interact antagonistically in dental epithelia to regulate the root lineage differentiation and EMT. These findings will aid in the design of new strategies to promote functional differentiation in the regeneration and tissue engineering of teeth and will provide new insights into the dynamic interactions between the Bmp and Wnt/β-catenin pathways during cell fate decisions.

The crowns of teeth of most mammals are covered by enamel, the hardest material in the body, which is produced by epithelium-derived ameloblasts and is essential for the chewing function of teeth. In contrast, the roots of teeth are covered by a much softer calcified tissue called cementum that is essential for the attachment of teeth to jawbones. There are two types of cementum: acellular cementum is found predominately on the coronal half of the root, and cellular cementum occurs more frequently on the apical half. Traditionally, both types of cementum are believed to be solely derived from the mesenchymal cells surrounding the tooth called dental follicle cells following the fragmentation of root epithelia (1). However, recent lineage-tracing research has indicated that some cementum-producing cells (cementoblasts) may originate from dental epithelial cells (2). The differentiation of ameloblasts starts once the tooth germ shape is determined around the so-called bell stage of embryonic tooth development, while the differentiation of the root epithelium cell lineage starts much later after birth in mice. At the initiation stage of differentiation of root epithelia, the dental epithelia extend apically to form a transient bilayered structure called Hertwig's epithelial root sheath (HERS). The HERS layers proliferate and extend apically and may guide the size, shape, and number of tooth roots by interacting with the dental mesenchyme through a Smad4-Shh-Nfic signaling cascade (3). Subsequently, HERS disintegrates into epithelial cell rests of Malassez (ERM) (1) and contributes to the formation of cementum either directly (2) or indirectly via secreted matrix proteins and signaling molecules (4).

The differentiation of dental epithelia in rodent incisors differs from that in other teeth: ameloblasts are exclusively on the labial surface analogous to the crowns, and the enamel-free lingual surface is analogous to the roots of the other teeth (5). Epithelial stem cell compartments are maintained at the apical ends of both sides of the incisors to enable their continuous growth (6). It has been proposed that epithelial dental stem cells can give rise to both ameloblasts and the root epithelium cell lineage and that the differentiation of the dental epithelial cells can be regulated independently from the regulation of stem cell maintenance (7).

It is generally accepted that, like the early stages of tooth development, the differentiation of dental epithelial cells is regulated via interactions between dental epithelial and mesenchymal cells. Bone morphogenetic protein (Bmp) signaling mediated by Bmp receptor type 1a (Bmpr1a)/activin receptor-like kinase 3 (Alk3) is essential for early tooth development by mediating the epithelial-mesenchymal interaction in a feedback circuit that involves the

Received 9 August 2013 **Returned for modification** 5 September 2013
Accepted 24 September 2013

Published ahead of print 30 September 2013

Address correspondence to Fei Liu, fliu@medicine.tamhsc.edu.

* Present address: Zhenhua Yang, Department of Orthodontics, School of Stomatology, Fourth Military Medical University, Xi'an, Shaanxi, China; Xinyu Ti, Xijing Hospital, Fourth Military Medical University, Xi'an, Shaanxi, China; Lei Shangguan, Xijing Hospital, Fourth Military Medical University, Xi'an, Shaanxi, China; Yanqiu Zhao, Lutheran Medical Center, Brooklyn, New York, USA; Julia Yu Fong Chang, Department of Oral & Maxillofacial Surgery (Oral Pathology), School of Dentistry, University of Washington, Seattle, Washington, USA.

Z.Y. and B.H. contributed equally to this article.

Supplemental material for this article may be found at http://dx.doi.org/10.1128/MCB.00456-13.

doi:10.1128/MCB.00456-13

Wnt/β-catenin pathway (8, 9). During the differentiation stage, Bmp signaling is linked to amelogenesis in continuously growing mouse incisors based on evidence from genetic manipulations of follistatin, an inhibitor of both Bmp and transforming growth factor β (TGF-β) pathways from the initiating stage of tooth development (10), but the direct roles of this pathway in amelogenesis in molars and the differentiation of the root epithelial lineage are unclear.

The aim of this study is to determine the direct roles of Bmp signaling in differentiation of dental epithelia. By depletion of epithelial Bmpr1a from the differentiation stage of tooth development in an inducible transgenic mouse model, we show here that the cessation of Bmp signaling promotes the differentiation of crown epithelia into the root lineage or even cementoblast-like cells instead of ameloblasts. This phenotype is accompanied by an epithelial-mesenchymal transition (EMT) and is dependent on the upregulation of Wnt/β-catenin signaling. Consistently, β-catenin depletion in dental epithelia significantly inhibited EMT and the differentiation into cementoblast-like cells. For the first time, we reveal the direct and essential roles of the Bmp-Wnt interaction in the cell fate decision of dental epithelia and the EMT regulation *in vivo*.

MATERIALS AND METHODS

Animals. Mice carrying the *Keratin5* (*Krt5*)-*rtTA* (11) and *tetO-Cre* (12) transgenes and the floxed *Bmpr1a* alleles (13) with or without the Rosa26R allele or the floxed *Ctnnb1* alleles (14) were placed on doxycycline (Dox) chow (6 g/kg of body weight; Bio-Serv, USA) to induce gene knockout or transgene expression. All animal procedures were performed under a protocol approved by the IACUC committees of Texas A&M Health Science Center (TAMHSC) and Scott & White Hospital.

Histology, X-Gal staining, immunohistochemistry, and *in situ* hybridization. Tissue preparation, histology, immunohistochemistry (IHC), immunofluorescence (IF) staining, *in situ* hybridization (ISH) with digoxigenin-labeled probes and 5-bromo-4-chloro-3-indolyl-β-D-galactopyranoside (X-Gal) staining were performed as previously described (2, 15). The following antibodies were used for IHC or IF: Krt5 (ab5312; Abcam) (1:200), Krt14 (ab130102; Abcam) (1:1,000), Alk3 (LS-C97656; Life Span) (1:100), phospho-Smad1/5/8 (catalog no. 9511; Cell Signaling) (1:100), β-catenin (C7207; Sigma) (1:500), Bsp (bs-2668R; Bioss) (1:200), collagen I (AB755P; Millipore) (1:1,000), N-cadherin (04-1126; Millipore) (1:100), vimentin (ab45939; Abcam) (1:500), phospho-Smad2 (AB3849; Millipore) (1:500), and phospho-Smad3 (ab51451; Abcam) (1:200).

Backscatter scanning electron microscopy and micro-computed tomography analysis. Backscatter scanning electron microscopy (SEM) was performed as previously reported (16). The micro-computed tomography (μCT) imaging of samples was performed with a Skyscan-1174 scanner (SKYSCAN, Belgium), and the data were analyzed with OsiriX imaging software (Pixmeo, Geneva, Switzerland) as previously described (17).

Isolation and differentiation of incisor epithelial stem/progenitor cells. Incisor epithelial stem/progenitor cells were isolated from the apical ends of incisors from postnatal day 7 (P7) mice by incubation in 1 mg/ml dispase and 1 mg/ml collagenase in phosphate-buffered saline (PBS) for 30 min at 37°C with shaking and cultured in the progenitor cell targeted oral epithelial medium CnT-24 (Zen-Bio, USA). The nonepithelial cells were depleted using three rounds of differential digestion with trypsin and 2 weeks of selective culture in CnT-24. The remaining epithelial cells were placed in Matrigel (BD, USA) in CnT-24 to expand into spheres. Subsequently, in the presence of 1 μg/ml doxycycline, these sphere cells were induced to differentiate in a 1:1 mixture of CnT-32 epithelial differentiation medium (Zen-Bio, USA) and filtered conditioned medium from the primary culture of apical-end cells mentioned above. Some cells were treated with TGF-β signaling inhibitor SB431542 (Sigma) (10 μM). For IF, cells were mounted on poly-L-lysine-coated coverslips. After 7 days of Dox induction, *in vitro* mineralization and collagen synthesis of dental epithelial stem/progenitor cells (DEpSCs) were induced under conditions optimized for the cementoblast cell line OCCM.30 and quantified as reported previously (18).

Quantitative reverse transcription-PCR analysis and statistics. Quantitative reverse transcription-PCR (qRT-PCR) analysis of mRNA was performed as previously reported (19) with primers from PrimerBank (http://pga.mgh.harvard.edu/primerbank). qRT-PCR analysis of microRNAs was performed with TaqMan microRNA assays (Applied Biosystems, USA).

Western blotting. Nuclear and cytoplasmic proteins were extracted from DEpSCs with NE-PER reagents containing inhibitors of protease and phosphatase (Pierce, USA). Western blotting was done as reported previously (19) with antibodies for β-catenin (Sigma) (1:2,000), phospho-Smad2 (Millipore) (1:1,000), phospho-Smad3 (Abcam) (1:1,000), and lamin A (Thermo Scientific) (1:200).

Statistics. All quantified data were analyzed using one-way analysis of variance (ANOVA) followed by Tukey's multiple-comparison test with GraphPad Prism software. A P value of <0.05 is considered to be significant.

RESULTS

Epithelial Bmpr1a/Alk3 knockout during the differentiation stage caused enamel defects and the formation of ectopic cellular cementum-like structures on tooth crowns. Bmpr1a/Alk3 is strongly expressed in the dental epithelia during the differentiation stage (20). To block epithelial Bmp signaling during this stage, we used the *Keratin5* (*Krt5*)-*rtTA* (11) and *tetO-Cre* (12) system to deplete epithelial *Alk3* upon induction with doxycycline (Dox) from embryonic day 14.5 (E14.5), approximately 1 day before the initiation of dental epithelial differentiation. In postnatal day 7 (P7) teeth of *Krt5-rtTA*/*tetO-Cre*/*Rosa26R* mice induced with Dox starting on E14.5, the expression of Cre reporter LacZ was detected by X-Gal staining in most dental epithelial cells, including ameloblasts and basal epithelia but not in cells of any other lineages (see Fig. S1A and B in the supplemental material), which verified the efficiency and specificity of Cre-mediated DNA recombination in this system. Double immunofluorescence (IF) staining of P7 teeth of *Krt5-rtTA*/*tetO-Cre*/*Alk3*$^{fl/fl}$ mice induced with Dox from E14.5 (*Alk3* knockout [AKO]) indicated that the expression of phospho-Smad1/5/8 in Krt14^{+} basal epithelial cells of both molar crowns and incisor crown analog was clearly decreased compared to that in wild-type (WT) crown tissues (see Fig. S1I to L).

In P42 AKO teeth, micro-computed tomography (μCT) imaging (Fig. 1A) and backscatter scanning electron microscopy (SEM) (Fig. 1B) indicated that the enamel formation in both molars and incisors was severely impaired. The crowns of the AKO molars were rough and covered by porous structures with low radiopacity in many regions when observed by SEM (arrow in Fig. 1B). These porous structures had no blood supply (Fig. 1C) and were closely attached to dentin, which are unique features of cellular cementum compared with bone. At the labial side of AKO incisors, the enamel was absent, and the dentin was fragmented in many places (Fig. 1A). The dentin of incisors was remarkably and irregularly thickened, which made pulp chambers much narrower and distorted (Fig. 1A and B). The histology of decalcified teeth was examined by Masson's trichrome (TRI) staining, which produces red stains on cells and preenamel and blue stains on colla-

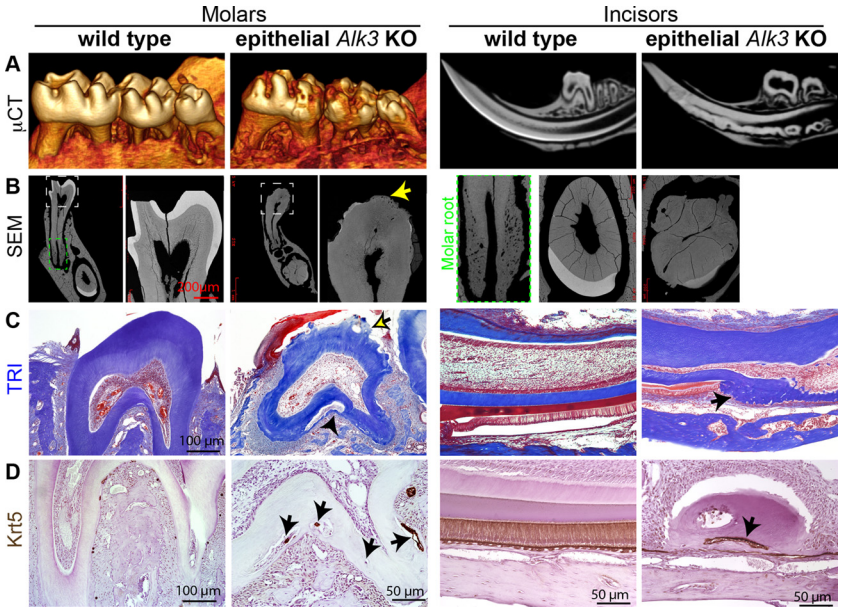

FIG 1 Radiological and histological analyses of enamel defects and ectopic cellular cementum-like structures in AKO teeth. *Krt5-rtTA/tetO-Cre/Alk3*$^{fl/fl}$ (*Alk3* KO [AKO]) mice and wild-type (WT) littermates were induced with Dox starting on E14.5. (A and B) Tooth samples were collected on P42 for μCT imaging (A) to examine molar surfaces or sagittal tooth sections or for backscatter SEM to show ultrastructures (B) with the green-outlined insert depicting the cellular cementum in a WT molar. (C and D) Sections of decalcified teeth were analyzed with TRI staining (C) or Krt5 IHC (D).

gen-abundant structures, including dentin and cementum. Decalcification removed the enamel completely and left smooth surfaces of crown dentin in wild-type molars, but the crown dentin in AKO molars was covered with small pits and blue-stained irregular prominences (Fig. 1C). Notably, the cementum in AKO molar roots appeared much thicker than that in WT roots and was separated from dentin at multiple places with many Krt5$^+$ cells embedded between (Fig. 1C and D). At the labial sides of the AKO incisors, the red-stained ameloblasts and preenamel were replaced in many regions by blue-stained and cell-containing irregular substances that appeared similar to the cellular cementum in molar roots of wild-type mice (Fig. 1C). Similar to that in AKO molar roots, many of these embedded cells in AKO incisors were Krt5$^+$ (Fig. 1D), suggesting that epithelium-originated cells might directly contribute to the formation of ectopic cementum-like structures as well as to the enhanced orthotopic cementogenesis. The apoptosis of root epithelia was not significantly affected by Alk3 depletion as indicated by terminal deoxynucleotidyltransferase-mediated dUTP-biotin nick end labeling (TUNEL) staining (see Fig. S2A in the supplemental material). However, proliferation was increased in root epithelial region of AKO teeth as indicated by IHC for proliferating cell nuclear antigen (PCNA) (see Fig. S2B), which is consistent with the report that Bmp4 inhibited proliferation and elongation of HERS (21) and the enhanced epithelium-originated cementogenesis in AKO teeth.

To determine the identity of these ectopic cementum-like structures in AKO mice, we collected tooth samples on P7 or P14 when crown epithelia on WT molars are still present. *In situ* hybridization (ISH) assays confirmed the effective depletion of *Alk3* mRNA and the significant downregulation of *Msx2*, a Bmp-regulated transcription factor essential for amelogenesis (22), in the crown epithelia of P7 AKO mice (Fig. 2A, B, and E to H). *Amelogenin* (*Amelx*) is a marker of ameloblasts and is regulated by the Bmp-Msx2 pathway. ISH indicated that *Amelx* was highly expressed in labial incisor epithelia (except for the cervical loop) and the molar crown epithelia in P7 WT mice but was absent in the majority of crown epithelia from P7 AKO mice (Fig. 2C and D). *α1 type I Collagen* (*Col1a1*) is expressed by both cementoblasts and dentin-producing odontoblasts, whereas *Bone sialoprotein* (*Bsp*) is expressed by cementoblasts and osteoblasts. In P7 or P14 samples, both markers were absent in the epithelia on the molar crowns and the labial side of incisors in WT mice but were strongly expressed in many cells at both locations in AKO mice (Fig. 2I to P), verifying the ectopic cementogenesis in tooth crowns of AKO mice.

Alk3 knockout in crown epithelia switched their differentiation into the root lineage and cementoblast-like cells and promoted the epithelial-mesenchymal transition. To explore the mechanism of ectopic cementogenesis in AKO mice, we examined the morphology of crown epithelia by ISH or IHC for Krt14 in tooth samples of P7 and P14 AKO mice induced from E14.5. In many places of the molar crown and the labial side of incisors in P7 AKO mice, the brush-shaped *Krt14*$^+$ ameloblasts were replaced by layers of flat *Krt14*$^+$ cells similar to HERS (Fig. 3A, orange arrowheads). On P14, when Krt14$^+$ epithelial cell rests of Malassez (ERM) are formed at the lingual side of WT incisors and around roots of WT molars, fragmented Krt14$^+$ cell clusters were present at the labial side of AKO incisors and on crowns of AKO molars in addition to root regions (Fig. 3B, orange arrowheads). The precocious fragmentation of dental epithelia appears not to be caused by apoptosis, since no obvious apoptosis was found in AKO dental epithelia (see Fig. S2A in the supplemental material). Notably, the ERM-like Krt14$^+$ cell clusters around roots of AKO molars were significantly enlarged compared to ERM in WT roots (Fig. 3B), which is related to increased proliferation of root epithelial cells

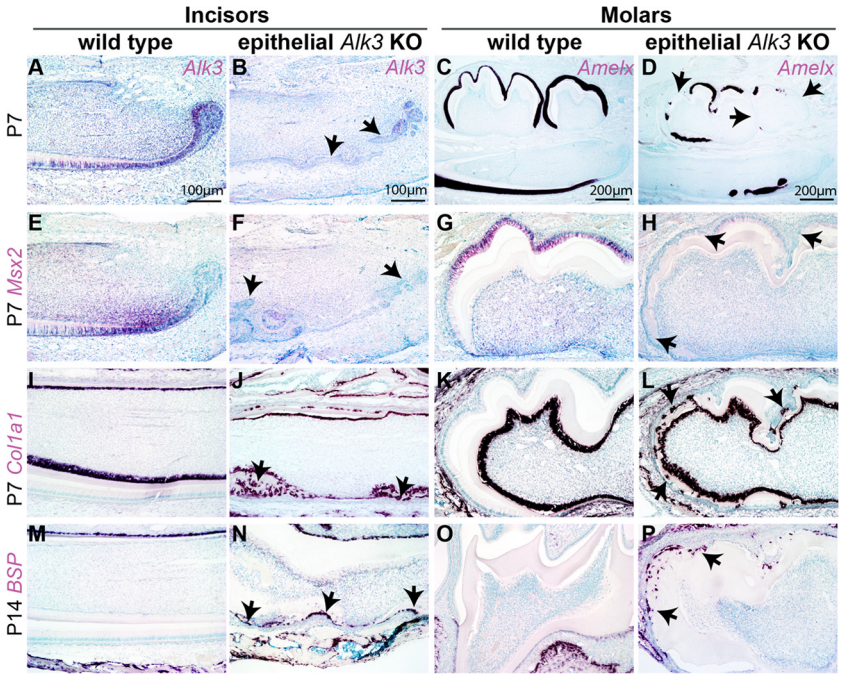

FIG 2 *In situ* hybridization for markers of ameloblasts and cementoblasts in AKO teeth. (A to P) Tooth samples were collected from WT and AKO mice induced from E14.5 on P7 (A to L) or P14 (M to P) for ISH of *Alk3* (A and B), the ameloblast marker *Amelx* (C and D), the Bmp target gene *Msx2* (E to H), and cementoblast markers *Col1a1* (I to L) and *Bsp* (M to P). Panels E to P have the same magnification as panels A and B.

(see Fig. S2B) and might contribute to the thickened cementum containing Krt5$^+$ cells in AKO molar roots (Fig. 1C and D).

In both human and mouse teeth, some cells in the intact HERS coexpress epithelial markers and mesenchymal markers such as N-cadherin (N-cad) and vimentin (Vim) (23, 24), which suggest the possibility of epithelial-mesenchymal transition (EMT) in HERS during root development. In AKO teeth, we noticed that many *Krt14*$^+$ dental epithelial cells on the molar crowns and at the labial side of incisors invaginated toward or into the dental pulps (Fig. 3A, black arrows). Double IF staining detected the expression of N-cad and Vim in some Krt14$^+$ crown epithelia of AKO teeth but not in that of WT teeth (Fig. 3C and D). Meanwhile, IF staining indicated that the expression of E-cadherin in basal epithelia of AKO tooth crowns was much lower than that in corresponding WT cells (Fig. 3E). Collectively, these data indicated the differentiation of AKO crown epithelia into the root lineage and also suggested the EMT in AKO crown epithelia.

It has also been suggested that some HERS cells undergo an EMT to become cementoblasts based on *in vitro* and *ex vivo* data (23, 25–27). In AKO tooth crowns at various stages, some Krt14$^+$ or Krt5$^+$ cells were embedded within calcified materials (green arrow in Fig. 3A and arrows in Fig. 1D). Double IF staining indicated that in WT teeth, collagen I (Col1) protein was expressed in dentin, cementum, and mesenchymal cells but not in Krt14$^+$ cells (Fig. 3F), whereas Bsp protein was expressed in cementum adjacent to Krt14$^+$ ERM cells but not in crown epithelia (Fig. 3G). In crowns of AKO teeth, the expression of Col1 and Bsp was colocalized or adjacent to Krt14$^+$ cells embedded within hard materials (Fig. 3F and G), suggesting the differentiation of some AKO crown epithelia to cementoblast-like cells.

To determine the origin of ectopic cementoblasts in AKO mice, we introduced the *Rosa26R* (*R26R*) reporter into the AKO strain to label the progeny of *Alk3*-depleted epithelial cells with *lacZ* expression. In sections of P7 and P14 AKO/R26R teeth induced with Dox from E14.5, X-Gal staining indicated that most crown *lacZ*$^+$ cells were flat basal epithelia, whereas residual column-shaped cells with the typical ameloblast morphology were mostly *lacZ*$^-$ cells (see Fig. S1C to H in the supplemental material), suggesting the inhibition of amelogenesis by Alk3 depletion is likely to be cell autonomous. Many crown *lacZ*$^+$ cells invaginated or immigrated into the calcified tissues or dental pulps (see Fig. S1C to F, black arrows). Particularly, some pieces of calcified tissues were surrounded only by *lacZ*$^+$ cells but not by *lacZ*$^-$ cells (see Fig. S1E, black arrowhead), suggesting epithelium-originated cementogenesis. However, the majority of cells embedded in these ectopic cementum-like structures were *lacZ*$^-$ cells, and both the crown dentin and the crown epithelial layer were fragmented at multiple locations (Fig. 3B; also see green arrows in Fig. S1E to H), suggesting that most of these ectopic cementoblast-like cells were originated from the mesenchymal cells from dental pulp or dental follicle.

Alk3 depletion in isolated incisor dental epithelial stem cells similarly promoted EMT and differentiation into the root lineage and cementoblast-like cells. To further determine the identity of AKO dental epithelia, we isolated dental epithelial stem/progenitor cells (DEpSCs) from the apical ends of incisors of WT or noninduced *Krt5-rtTA*/*tetO-Cre*/*Alk3*$^{fl/fl}$ mice (Fig. 4A) with a method established recently (28). IF staining indicated that most isolated cells were Krt14$^+$ (Fig. 4B) (98.6% ± 0.5% Krt14$^+$ cells [mean ± standard error of the mean], $n = 3$). Quantitative RT-PCR (qRT-PCR) indicated that the mRNA copy number ratio of the epithelial marker *Krt5* and the mesenchymal marker *Vim* in the isolated cells was dramatically higher than that in cultured primary incisor apical-end cells containing both cell types

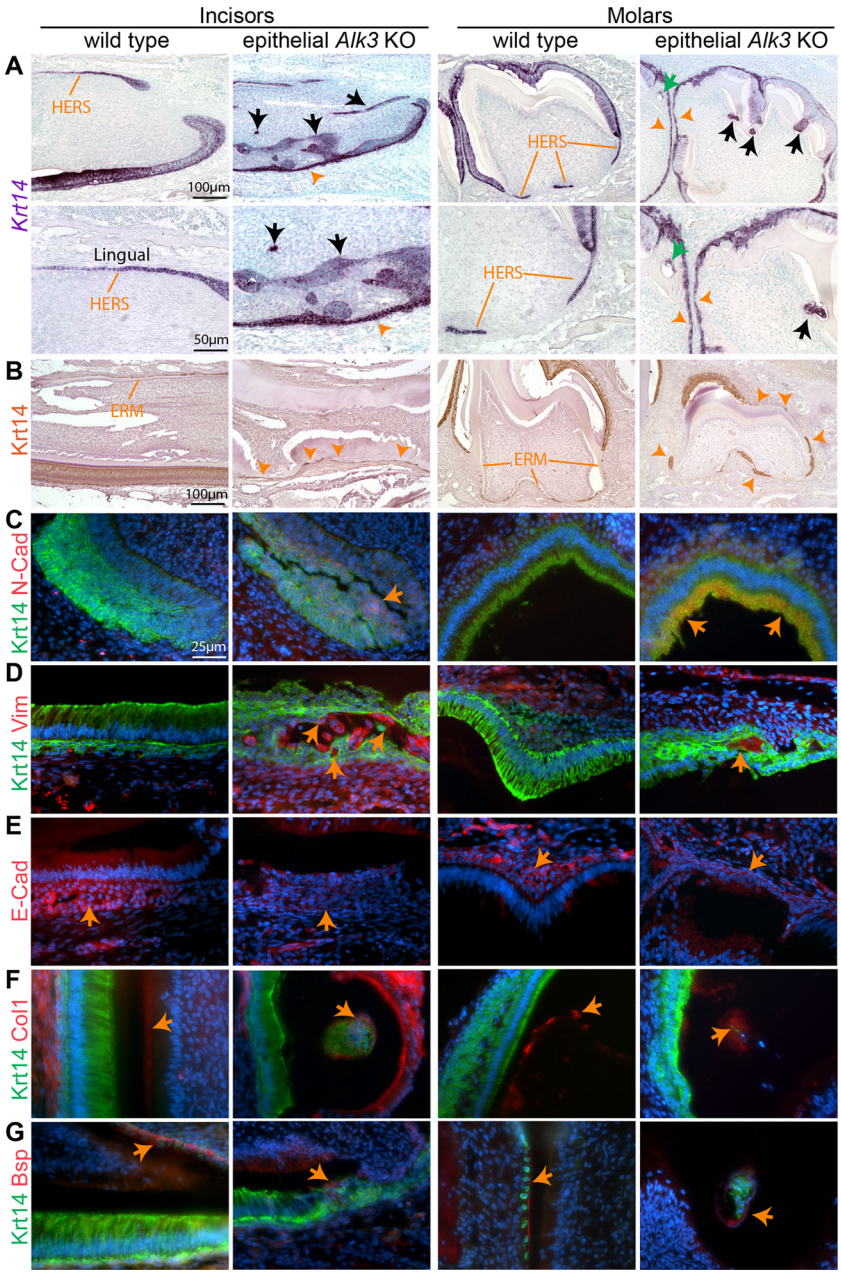

FIG 3 Morphology and differentiation of dental epithelia in AKO teeth. (A to G) P7 and P14 tooth samples were collected from WT and AKO mice induced from E14.5 for ISH or IHC of Krt14 (A and B) or double immunofluorescence staining of Krt14 and N-cadherin, vimentin, E-cadherin, collagen I or Bsp (C to G). The nucleus was counterstained with 4′,6′-diamidino-2-phenylindole (DAPI) (blue) in panels C to G.

(Fig. 4C) ($P < 0.0001$, $n = 3$), further confirming the efficient depletion of mesenchymal cells by this method. Compared to WT DEpSCs before differentiation, in WT cells cultured for 7 days with differentiation medium containing Dox, the expression of stem cell markers *Bmi1* (29) and c-*Kit* was significantly downregulated, whereas the expression of ameloblast markers *Amelx* and *Msx2* and mesenchymal markers *N-cad* and *Vim* was all significantly upregulated (Fig. 4D) ($P < 0.01$, $n = 3$), suggesting that these DEpSCs could give rise to both the ameloblast and root epithelium lineage under this differentiation condition as proposed (7).

Compared to WT cells after differentiation, in similarly treated AKO cells, the expression of *Alk3* and *Msx2* was significantly decreased, which confirmed the efficient blockade of Bmp signaling in these cells. In differentiated AKO cells, the expression of *Amelx* and *E-cad* was significantly decreased, whereas the expression of *N-cad*, *Vim*, and the cementoblast markers *Col1a1* and *Bsp* was significantly increased (Fig. 4E) ($P < 0.01$, $n = 3$), consistent with the differentiation of crown epithelia toward HERS and cementoblast-like cells instead of ameloblasts observed *in vivo*. qRT-PCR also revealed the significant upregulation of multiple pro-EMT factors, including *Matrix metallopeptidase 2* (*Mmp2*), *Periostin*

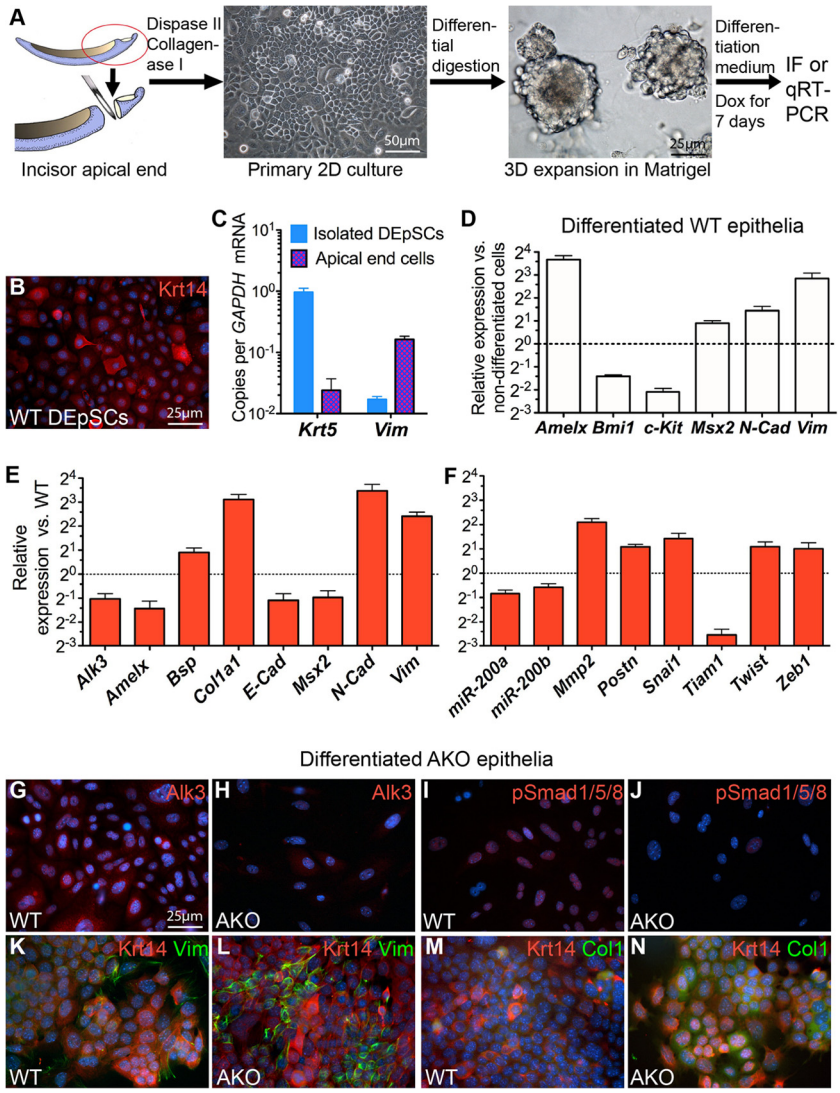

FIG 4 Effects of Alk3 depletion on expression of differentiation markers and EMT-related genes in cultured dental epithelia. (A to N) Dental epithelial stem cells (DEpSCs) were isolated from the apical ends of incisors of P7 AKO and WT mice that were not exposed to Dox, expanded as spheres, and induced to differentiate in the presence of Dox for 7 days (A) for qRT-PCR (C to F), IF staining of Krt14 (B), Alk3 (G and H), or phospho-Smad1/5/8 (pSmad1/5/8) (I and J), or double IF staining for Krt14 and vimentin (K and L) or collagen I (M and N). The error bars in panels C to E show standard errors of the means (error bars) ($n = 3$ and $P < 0.05$ for all genes examined). 2D, two-dimensional.

(*Postn*), *Snai1*, *Twist*, and *Zeb1* (30) in AKO cells (Fig. 4F) ($P <$ 0.01 for all genes, $n = 3$). Conversely, the expression of the EMT inhibitor *Tiam1*, a gene required for adherens junction maintenance (31), was significantly decreased in AKO cells (Fig. 4F) ($P <$ 0.01, $n = 3$). Meanwhile, the expression of *miR-200a* and *miR-200b*, microRNAs that are induced by Bmp signaling (32) and are essential for stabilizing the epithelial state and inhibiting the EMT by targeting pro-EMT factors (33), was also significantly downregulated in AKO cells (Fig. 4F) ($P < 0.01$, $n = 3$). The efficient depletion of Alk3 protein and the inhibition of Bmp signaling in cultured AKO epithelia were further verified by IF staining for Alk3 and phospho-Smad1/5/8 (Fig. 4G to J). Double IF staining indicated that Vim and Col1 were expressed in a few Krt14$^+$ WT dental epithelia and many more Krt14$^+$ AKO cells, which confirmed that the upregulation of these genes by epithelial *Alk3* depletion did happen in epithelia and was not a secondary effect caused by residual mesenchymal cells in the culture (Fig. 4K to N). IF staining also indicated the relocation of β-catenin protein from membrane to cytoplasm and nucleus in AKO cells compared to WT cells (Fig. 5C). Taken together, we detected all 5 types of markers for EMT (34) in AKO cells, including cell surface proteins (downregulation of *E-cad* and upregulation of N-cad), cytoskeletal markers (upregulation of Vim and relocation of β-catenin), extracellular matrix (ECM) proteins (upregulation of *Col1*, *Bsp*, *MMP2* and *Postn*), transcription factors (upregulation of *Snai1*, *Twist*, and *Zeb1*), and microRNAs (downregulation of *miR-200a/b*), confirming the promotion of EMT in dental epithelia by Alk3 depletion.

To examine the potential of DEpSCs to differentiate into cementum-producing cells, we examined *in vitro* mineralization and collagen synthesis of these cells with conditions optimized for the cementoblast cell line OCCM.30 (18). von Kossa staining and

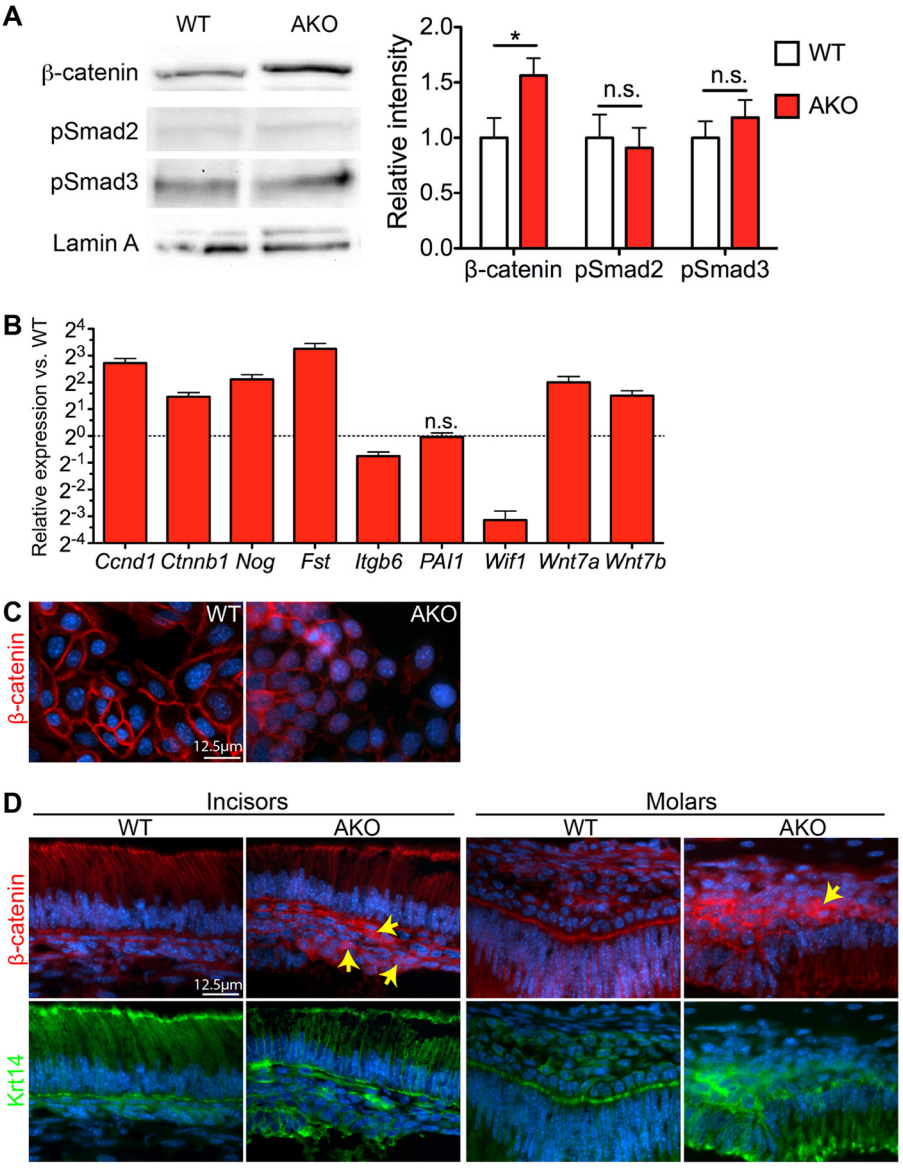

FIG 5 Depletion of Alk3 in dental epithelial upregulated activity of Wnt/β-catenin signaling but not that of TGF-β signaling. (A to C) AKO and WT DEpSCs were induced as described in the legend to Fig. 4 and analyzed by Western blotting of nuclear proteins (A), qRT-PCR (B), or IF (C) to examine the expression of genes related to the Wnt/β-catenin pathway or the TGF-β pathway ($n = 3$ in each assay) (n.s., not significant; *, $P < 0.05$). (D) P7 WT and AKO teeth were examined with double IF for β-catenin and Krt14.

quantitative calcium assay indicated that AKO but not WT DEpSCs were capable of producing a few mineral nodules with detectable calcium incorporation after culture under this condition for 14 days (see Fig. S3A in the supplemental material), whereas Picrosirius red staining and quantitative collagen assay indicated that collagen synthesis was detected in WT DEpSCs and was significantly increased in AKO DEpSCs (see Fig. S3B). These data suggested that WT DEpSCs have limited potential to produce cementum, but this potential was significantly increased in AKO DEpSCs.

Epithelial Alk3 knockout promoted the Wnt/β-catenin signaling. Bmpr1a depletion in the kidney tubular epithelium enhances TGF-β1–Smad3 signaling and the EMT (35), but we did not find significant upregulation of TGF-β/Smad signaling activity in cultured AKO dental epithelia compared to WT cells as indicated by Western blotting for phospho-Smad2 or phospho-Smad3 (Fig. 5A) and by qRT-PCR analysis of the TGF-β target genes *PAI1* and *Itgb6* (36) (Fig. 5B). However, inhibiting TGF-β signaling in AKO DEpSCs with SB431542 significantly repressed the upregulation of mesenchymal markers (*N-cad* and *Vim*), some pro-EMT factors (*Mmp2*, *Postn*, and *Zeb1*), and cementoblast markers (*Bsp* and *Col1a1*) by Alk3 depletion but did not significantly affect the downregulation of *Amelx*, *Ecad*, and *Tiam1* and the upregulation of other pro-EMT factors (*Snai1* and *Twist*) by Alk3 depletion (see Fig. S4 in the supplemental material). These data suggested that the basal level of TGF-β signaling activity is required for the EMT and differentiation switch of AKO dental epithelia but is not the cause of these events.

Wnt/β-catenin signaling is essential for the EMT by upregulating pro-EMT transcription factors such as Snai1 and Twist (37). Bmp/Smad4 signaling negatively regulates Wnt/β-catenin signaling in lung epithelial cells by inducing the Wnt inhibitor Wif1 (38), in hair bulge epithelial stem cells by inhibiting the expression of Wnt7a and Wnt7b (39), in intestinal epithelial cells by directly inhibiting transcription of the β-catenin gene (40), or in nasopharyngeal carcinoma cells by inducing miR-200a to suppress β-catenin translation (41). Western blotting and qRT-PCR assay indicated that the level of nuclear β-catenin protein and mRNA (*Ctnnb1*) in AKO dental epithelia was significantly upregulated (Fig. 5A and B). Nuclear translocation of β-catenin was observed by IF in cultured AKO DEpSCs (Fig. 5C) and in some $Krt14^+$ basal epithelial cells on AKO tooth crowns (Fig. 5D, arrows), indicating activation of the Wnt/β-catenin pathway. Consistent with findings in other epithelial cells, in AKO cells the expression of Wnt inhibitor *Wif1* was significantly downregulated, whereas the expression of Wnt ligands *Wnt7a* and *Wnt7b* and Wnt target genes, including *Cyclin D1* (*Ccnd1*) (42), *Follistatin* (*Fst*) (43), and *Noggin* (*Nog*) (44), was significantly upregulated (Fig. 5B) ($P < 0.01$, $n = 3$). In addition, the upregulation of *Postn* and the downregulation of E-cad and *Tiam1* (Fig. 4E and F) in AKO dental epithelia also contributed to the upregulation of Wnt/β-catenin signaling by recruiting Wnt ligands (45) and releasing β-catenin from adhesion complexes (37), respectively. Other mechanisms such as decreased sequestration of Dvl-1 from the Wnt signaling cascade by phosphorylated Smad1 (46) might also be involved. Collectively, these data indicated that the depletion of Alk3 in dental epithelia leads to upregulation of Wnt/β-catenin signaling.

Epithelial β-catenin knockout led to defects of enamel and root shape without ectopic cementogenesis *in vivo* and inhibited EMT and cementogenesis *in vitro*. To examine the roles of epithelial Wnt/β-catenin signaling in differentiation of dental epithelia, we generated *Krt5-rtTA/tetO-Cre/Ctnnb1*$^{fl/fl}$ inducible β-catenin knockout (BKO) mice by crossing the mice and induced them with Dox from E14.5. On P42, obvious enamel defect was found in some molars and incisors (7 of 24 [29.2%]) of BKO mice by μCT scanning, but the degrees were highly variable even in samples from the same mouse possibly due to fluctuant efficiency of depleting β-catenin (see Fig. S5B in the supplemental material). In most severely affected P42 BKO teeth, μCT scanning and backscatter SEM indicated that the labial enamel in incisors had disappeared, whereas the labial dentin was fragmented; similarly, the enamel in molar crowns was absent or much thinner in many regions (Fig. 6A and B). At the labial side of these BKO incisors, TRI staining indicated that red-stained ameloblasts and preenamel were absent (see Fig. S5A in the supplemental material), whereas IHC for Krt5 indicated fragmentation of labial epithelia similar to that at the lingual side in 2 of 6 incisors examined (Fig. 6E, arrows), which might be related to fragmentation of labial dentin. Meanwhile, μCT scanning indicated that the shape of all molar roots in BKO mice was distorted and the bifurcation of roots was absent in most second and third molars (Fig. 6A and F, $n = 18$).

In P7 BKO samples induced from E14.5, ISH indicated that the expression of *Ctnnb1* was absent from part of the dental epithelia and downregulated in much larger regions due to variable recombination efficiency of the Cre/loxp system (see Fig. S5B in the supplemental material). Dlx3 and Msx2 are transcription factors required for amelogenesis (47) and regulated by the Wnt/β-catenin pathway (48, 49). ISH of serial sections indicated that the expression of these two factors and *Amelx* was significantly downregulated in *Ctnnb1*-negative epithelia in both molars and incisors (Fig. 6C; see also Fig. S5C and D), suggesting that the Wnt/β-catenin pathway is required for proper amelogenesis. However, consistent with the lack of ectopic cellular cementum-like structures in P42 BKO teeth, expression of *Col1a1* was not detected in *Ctnnb1*-negative epithelia of P7 BKO tooth (Fig. 6D). Proliferation and apoptosis were not significantly affected in BKO root epithelia (see Fig. S2 in the supplemental material), whereas *Krt14* ISH indicated precocious fragmentation of root dental epithelia in 8 of 12 P7 BKO molars examined (Fig. 6E, arrows), which might be related to the later root phenotype in BKO mice. This phenotype might be due either to impaired Wnt/β-catenin signaling or to adhesion defects.

qRT-PCR assay of DEpSCs from WT and BKO samples confirmed downregulation of *Ctnnb1* and amelogenesis-related genes, including *Amelx*, *Dlx3*, and *Msx2* (Fig. 6G) ($P < 0.05$, $n = 3$). Interestingly, the expression of mesenchymal markers (*N-cad* and *Vim*), cementoblast markers (*Col1a1* and *Bsp*), and pro-EMT genes (*Snai1*, *Twist*, *Zeb1*, and *Postn*) in cultured BKO dental epithelia was also significantly decreased (Fig. 6G and H) ($P < 0.01$, $n = 3$), whereas the expression of epithelial marker *E-cad* was not significantly affected ($P > 0.05$), suggesting inhibition of EMT and epithelium-originated cementogenesis. Consistently, the collagen deposition by BKO DEpSCs was significantly decreased than that by WT cells (see Fig. S3B in the supplemental material). The expression of Wnt target gene *Tiam1* was significantly downregulated too ($P < 0.05$), which might contribute to fragmentation of dental epithelia by impairing maintenance of adherens junctions together with the depletion of β-catenin. In contrast to the upregulation of *Fst* and *Nog* in AKO cells, in BKO cells, the expression of *Fst*, *Nog*, and another secreted inhibitor of Bmp and Wnt pathways, *Sostdc1* (50), was significantly decreased, whereas the expression of *Bmp receptor 1b* (*Bmpr1b*/*Alk6*) was significantly upregulated (Fig. 6I) ($P < 0.01$, $n = 3$).

Taken together, these data suggested that Wnt/β-catenin signaling is required for both amelogenesis and EMT of dental epithelia.

Concomitant depletion of β-catenin rescued the EMT and ectopic cementogenesis caused by Alk3 depletion. To determine whether the EMT and consequent ectopic cementogenesis caused by Alk3 depletion is dependent on the upregulation of β-catenin signaling, we generated *Krt5-rtTA/tetO-Cre/Alk3*$^{fl/fl}$/*Ctnnb1*$^{fl/fl}$ inducible compound knockout (CKO) mice and induced them with Dox starting on E14.5. μCT scanning and TRI staining showed mild enamel defects in some P42 CKO teeth, but the ectopic cellular cementum-like structures were not observed (Fig. 7A to D compared to corresponding data of WT and AKO teeth in Fig. 1A and C). Proliferation and apoptosis were not significantly affected in CKO dental epithelia (see Fig. S2 in the supplemental material). ISH for *Krt14* indicated that in P7 CKO teeth, some column-shaped crown epithelial cells were replaced by flatter epithelia similar to that in AKO samples, but no invagination or immigration of $Krt14^+$ epithelia was observed (arrows in Fig. 7E and F compared to Fig. 3A), suggesting the absence of EMT. ISH of serial sections of CKO teeth for *Msx2*, *Amelx*, and *Col1a1* indicated that although the expression of *Msx2* and *Amelx* was significantly downregulated in some regions as in AKO samples (Fig. 7G to J compared to Fig. 2C to H), the expression of cementoblast marker

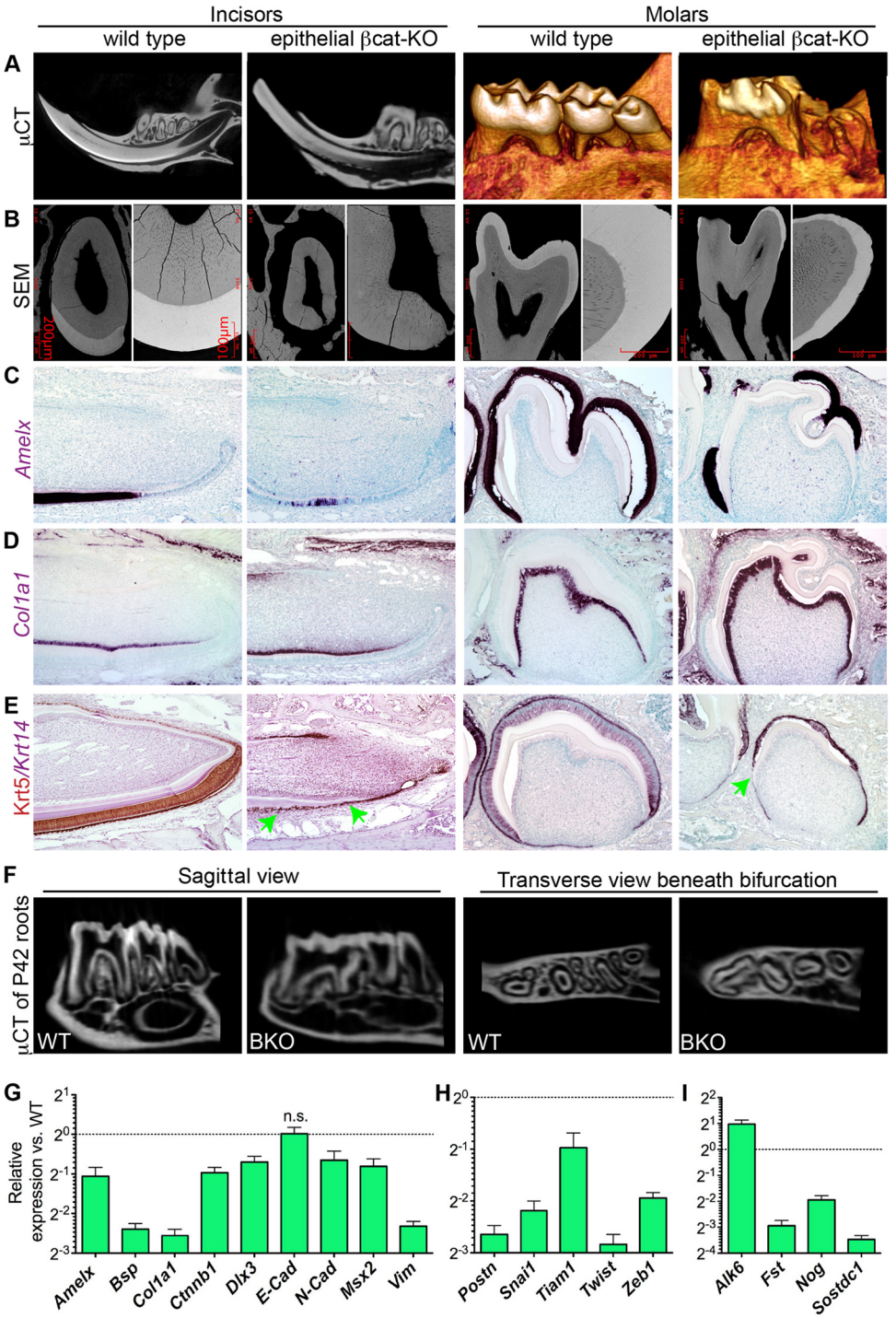

FIG 6 Effects of epithelial β-catenin (βcat) depletion on amelogenesis, EMT, and cementogenesis. P42 WT or BKO teeth were examined with μCT scanning (A and F), backscatter SEM (B), or IHC for Krt5 (E). P7 WT or BKO teeth were examined with ISH for *Amelx* (C), *Col1a1* (D), and *Krt14* (E). (G to I) WT and BKO DEpSCs were induced as described in the legend to Fig. 4 and analyzed with qRT-PCR for expression of genes related to amelogenesis or cementogenesis (G), EMT (H), and the Bmp pathway (I) ($n = 3$ and $P < 0.05$ for all genes except *E-cad*).

Col1a1 in these regions was not significantly upregulated as in AKO teeth (Fig. 7K and L compared to Fig. 2I to L), suggesting the absence of ectopic cementogenesis.

Tooth phenotypes and the penetrance of enamel defects (ED) or ectopic cellular cementum-like structures (ECC) in WT, AKO, BKO, and CKO mice at both P7 (16 lower teeth from 2 mice) and P42 (24 lower teeth from 3 mice) were summarized in Fig. 8A and B. Fisher's exact test indicated that the differences of ED penetrance at both P7 and P42 are significant between each group ($P < 0.05$) except that between BKO and CKO groups. The dif-

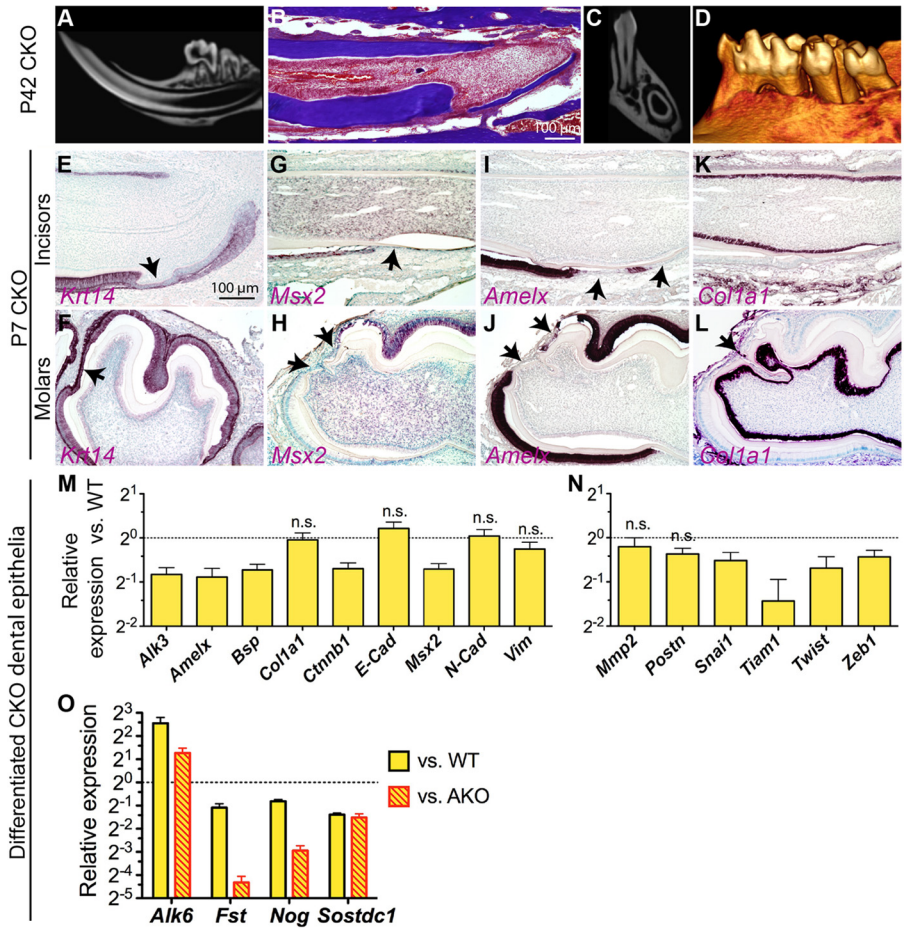

FIG 7 The EMT and ectopic cementogenesis caused by *Alk3* depletion is dependent on Wnt/β-catenin signaling. *Krt5-rtTA/tetO-Cre/Alk3*$^{fl/fl}$*/Ctnnb1*$^{fl/fl}$ compound knockout (CKO) mice were induced with Dox from E14.5. (A to D) P42 CKO tooth samples were analyzed with μCT imaging (A, C, and D) and TRI staining (B). (E to L) P7 CKO tooth samples were analyzed with ISH for *Krt14* (E and F), *Msx2* (G and H), *Amelx* (I and J), and *Col1a1* (K and L). Panels F to L are the same magnification as in panel E. (M to O) CKO and WT DEpSCs were induced as described in the legend to Fig. 4 and analyzed by qRT-PCR for the expression of genes related to differentiation (M), the EMT (N), and the Bmp pathway (O) ($n = 3$ and $P < 0.05$ for all genes not labeled with n.s.).

ferences of ECC penetrance are significant between AKO and all other groups ($P < 0.01$) and between the P7 CKO group and the P7 WT or BKO group ($P < 0.05$) but are not significant between the P42 CKO group and the P42 WT or BKO group ($P > 0.05$).

In cultured CKO dental epithelia, qRT-PCR (Fig. 7M) ($n = 3$) indicated that the levels of expression of *Alk3*, *Ctnnb1*, *Amelx*, *Msx2*, and *Bsp* were all significantly decreased ($P < 0.01$), whereas the expression of *Col1a1*, *E-Cad*, *N-Cad*, and *Vim* was not significantly changed ($P > 0.05$), suggesting that concomitant depletion of β-*catenin* and *Alk3* inhibited differentiation into ameloblasts but did not promote differentiation into the typical root lineage expressing mesenchymal markers or cementoblast-like cells. For EMT-related genes (Fig. 7N) ($n = 3$), although the expression of anti-EMT gene *Tiam1* was significantly downregulated ($P < 0.05$), the expression of pro-EMT genes was either not significantly affected (*MMP2* and *Postn*; $P > 0.05$) or even downregulated (*Snai1*, *Twist*, and *Zeb1*; $P < 0.05$), indicating the absence of EMT. Consistently, no significant difference in the formation of mineral nodules, calcium incorporation, and collagen deposition was observed between WT and CKO DEpSCs (see Fig. S3 in the supplemental material). Similar to that in BKO cells, in CKO cells, the expression of *Fst*, *Nog*, and *Sostdc1* was significantly decreased and that of *Bmpr1b*/*Alk6* was significantly upregulated compared to either WT or AKO cells (Fig. 7O) ($P < 0.01$, $n = 3$). Changes of these Bmp-related genes may contribute to the rescue of phenotypes caused by Alk3 depletion.

Collectively, these data showed that *Alk3* was sufficiently depleted in CKO dental epithelia, but the EMT and ectopic cementogenesis were rescued by the concomitant depletion of β-*catenin*, indicating that these effects of *Alk3* knockout are dependent on the upregulation of the Wnt/β-catenin pathway.

DISCUSSION

The molecular control of the differentiation of dental epithelia to the root lineage is unclear yet. In mouse incisors transplanted into kidney capsule, conventional knockout of fibroblast growth factor 10 (FGF10) leads to the loss of the dental epithelial stem cell compartment at the apical end of the crown analog (the labial side) and the transition from crown analog to root analog (51). However, it is not clear whether the disappearance of FGF10 regulates dental epithelium differentiation directly or only indirectly through disruption of the epithelial stem cell compartment. On the other side,

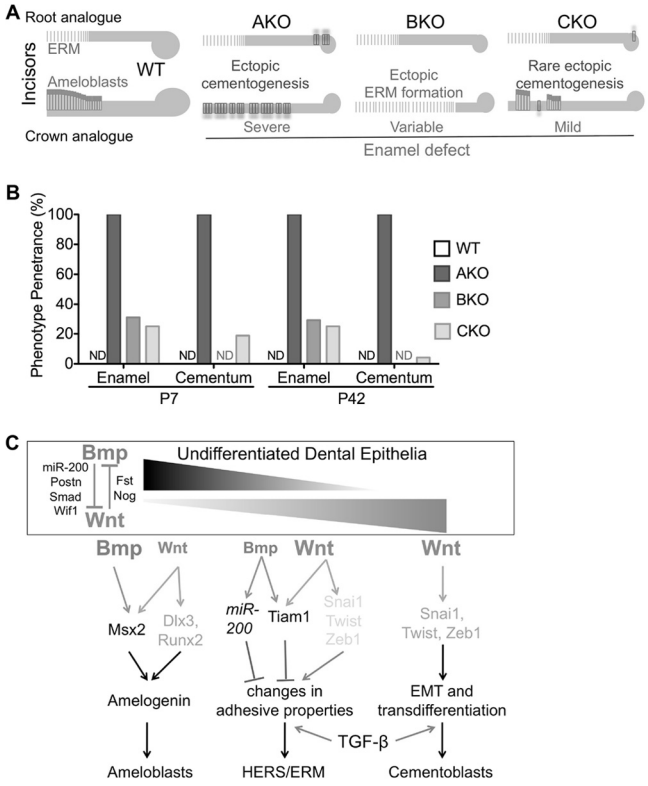

FIG 8 Schematic summary and hypothesis of roles of Bmp and Wnt signaling in the differentiation of dental epithelia. (A) Schematic summary of tooth phenotypes in WT, AKO, BKO, and CKO mice. (B) Penetrance of enamel defects or ectopic cellular cementum-like structures in these strains ($n = 16$ [P7] or 24 [P42]). ND, not detected. (C) Hypothesis on roles of Bmp and Wnt signaling in the differentiation of dental epithelia. Strong Bmp signaling in crown/labial dental epithelia collaborates with weak Wnt signaling to trigger amelogenesis. The balance of strong Wnt signaling and weak Bmp signaling in apical/lingual dental epithelia promotes formation of HERS/ERM via changes in adhesion properties. Cessation of Bmp signaling in dental epithelia promotes precocious formation of HERS/ERM and epithelium-originated cementogenesis via EMT mediated by upregulation of Wnt signaling. Basal TGF-β signaling activity is required for both HERS/ERM formation and EMT.

Bmp signaling is required for ameloblast differentiation of crown epithelia (10), but whether cessation of Bmp signaling is sufficient to induce differentiation of dental epithelia to the root lineage is unclear. Here we show that knockout of Bmpr1a/Alk3 in dental epithelia at the differentiation stage switched the fate of crown epithelia to the root lineage in a β-catenin-dependent manner, suggesting that cessation of epithelial Bmp signaling and/or upregulation of Wnt/β-catenin signaling are essential molecular switches to initiate differentiation of dental epithelia to the root lineage (Fig. 8C).

In support of our hypothesis, at E17.5 late bell stage, the expression of Bmp inhibitor Noggin is localized to the dental epithelium on the lingual side in the incisor (future root analog) and the external enamel epithelium of the molar (52) that was recently proposed to be the major source of HERS (53); in E18 incisors, at the lingual side, the expression of Bmp ligands is much lower, whereas the expression of Bmp/TGF-β inhibitor Fst is much higher than those at the labial side (10); in newborn mouse molars, Bmp ligands were detected in odontoblasts with seemingly lower intensity at the future apical end, whereas Fst was restricted to the cervical regions (54). On the other hand, the expression of Wnt reporter Axin2-LacZ concentrated around the developing roots (55), suggesting a high level of Wnt signaling activity in this region. Wnt10a and Wnt10b are highly expressed by differentiating odontoblasts before and during differentiation of root epithelia (17, 56). We found that DEpSCs also express Wnt7a and Wnt7b that was upregulated by Alk3 depletion. Hence, multiple Wnt ligands from both dental epithelial and mesenchymal cells might be involved in the differentiation to the root epithelial lineage.

It has been suggested that some HERS cells undergo EMT *in vivo* (23, 24) and that isolated root epithelial cells can differentiate into cementoblasts via EMT *in vitro* or *ex vivo* (23). Here we present the first *in vivo* evidence that some crown epithelia underwent EMT and differentiated into root lineage and cementoblast-like cells when epithelial Bmp signaling was blocked by the depletion of Bmpr1a. The role of Bmpr1a-mediated Bmp signaling in EMT appears to be context dependent: during human skin wound healing and mouse cardiac cushion development, Bmp2-Bmpr1a signaling promoted EMT (57, 58); conversely, during renal fibrosis, constitutively active Bmpr1a stimulated E-cad expression and reversed TGF-β1-induced EMT through direct antagonism (59), whereas Bmpr1a depletion in tubular epithelium enhanced TGF-β1–Smad3 signaling and EMT (35). Although TGF-β signaling activity was required for upregulation of pro-EMT factors and mesenchymal markers in AKO DEpSCs, it was Wnt/β-catenin, not TGF-β, signaling activity that was significantly upregulated by Alk3 depletion. The upregulation of Fst, an inhibitor of both TGF-β and Bmp pathways and a Wnt target gene, may contribute to the lack of upregulation of TGF-β signaling in AKO dental epithelia. Wnt/β-catenin signaling is essential for EMT in various contexts by the direct induction of multiple pro-EMT genes to repress E-cad expression or promote E-cad degradation (37). Concomitant depletion of β-catenin rescued the EMT and ectopic cementogenesis on tooth crowns caused by Alk3 depletion, indicating the dependence of these processes on β-catenin signaling.

The Bmp and Wnt/β-catenin pathways interact at multiple levels in various cellular contexts. At early stages of tooth morphogenesis, the Wnt-Bmp feedback circuit accounts for reciprocal epithelial-mesenchymal signaling interactions (9). Later, during odontoblast differentiation, Smad4-mediated inhibition of Wnt/β-catenin signaling controls the fate of cranial neural crest cells (60). Our data indicated that in dental epithelia at the differentiation stage, Bmp signaling inhibits Wnt/β-catenin signaling through multiple mechanisms, whereas Wnt/β-catenin signaling conversely represses Bmp signaling by induction of secreted inhibitors of Bmp/TGF-β pathways. As suggested by the disruption of labial cervical loops in P7 AKO incisors, the maintenance of incisor epithelial stem cells was also affected by the manipulation of the Bmp pathway, which is beyond the scope of this research. Nevertheless, the similar differentiation defects in molars and incisors of AKO mice suggested that the roles of Bmp signaling in the differentiation of incisor epithelial cells are similar to those in molars and are likely independent from its roles in the regulation of dental epithelial stem cells.

In *K14-Cre/Smad4*$^{fl/fl}$ tooth transplants, HERS enlarges but cannot elongate to guide root development (3). In our AKO mice induced from E14.5, despite the precocious formation and fragmentation of HERS-like structures on tooth crowns and the enlargement of the ERM-like structures in tooth roots, the elonga-

tion of orthotopic HERS and the shape, size, and number of roots were not significantly affected. These differences suggested that the TGF-β pathway, earlier effects of Bmp signaling, or some other unknown Smad4-mediated signaling in dental epithelia was sufficient to guide HERS elongation and root formation in the absence of Bmp signaling in HERS. Further experiments such as inducible knockout of TGF-β receptor in dental epithelia will help to clarify this issue.

In conclusion, our data suggested that the Bmp and Wnt/β-catenin pathways are mutually inhibitory in dental epithelia during the differentiation stage, and their interactions determine the differentiation of dental epithelia to ameloblasts, the root lineage, and probably cementoblasts. These findings will aid in the design of new strategies to promote functional differentiation in the regeneration and tissue engineering of teeth.

ACKNOWLEDGMENTS

This work is supported by start-up funding from Texas A&M Health Science Center.

We sincerely thank Adam Glick (Pennsylvania State University) for the *Krt5-rtTA* mice, Andras Nagy (Mount Sinai Hospital, Toronto, Canada) for the *tetO-Cre* mice, Richard Behringer (M. D. Anderson Cancer Center) for the *Bmpr1a*$^{fl/fl}$ mice, George Cotsarelis and Lewis A. Chodosh (University of Pennsylvania) for the *Ctnnb1*$^{fl/fl}$ and *tetO-Wnt1* mice, and Yang Chai (University of Southern California) for plasmid templates of probes for ISH.

REFERENCES

1. **Diekwisch TG.** 2001. The developmental biology of cementum. Int. J. Dev. Biol. **45:**695–706.
2. **Huang X, Bringas P, Jr, Slavkin HC, Chai Y.** 2009. Fate of HERS during tooth root development. Dev. Biol. **334:**22–30.
3. **Huang X, Xu X, Bringas P, Jr, Hung YP, Chai Y.** 2010. Smad4-Shh-Nfic signaling cascade-mediated epithelial-mesenchymal interaction is crucial in regulating tooth root development. J. Bone Miner. Res. **25:**1167–1178.
4. **Zeichner-David M.** 2006. Regeneration of periodontal tissues: cementogenesis revisited. Periodontol. 2000 **41:**196–217.
5. **Tummers M, Thesleff I.** 2003. Root or crown: a developmental choice orchestrated by the differential regulation of the epithelial stem cell niche in the tooth of two rodent species. Development **130:**1049–1057.
6. **Harada H, Kettunen P, Jung HS, Mustonen T, Wang YA, Thesleff I.** 1999. Localization of putative stem cells in dental epithelium and their association with Notch and FGF signaling. J. Cell Biol. **147:**105–120.
7. **Tummers M, Thesleff I.** 2008. Observations on continuously growing roots of the sloth and the K14-Eda transgenic mice indicate that epithelial stem cells can give rise to both the ameloblast and root epithelium cell lineage creating distinct tooth patterns. Evol. Dev. **10:**187–195.
8. **Andl T, Ahn K, Kairo A, Chu EY, Wine-Lee L, Reddy ST, Croft NJ, Cebra-Thomas JA, Metzger D, Chambon P, Lyons KM, Mishina Y, Seykora JT, Crenshaw EB, III, Millar SE.** 2004. Epithelial Bmpr1a regulates differentiation and proliferation in postnatal hair follicles and is essential for tooth development. Development **131:**2257–2268.
9. **O'Connell DJ, Ho JW, Mammoto T, Turbe-Doan A, O'Connell JT, Haseley PS, Koo S, Kamiya N, Ingber DE, Park PJ, Maas RL.** 2012. A Wnt-bmp feedback circuit controls intertissue signaling dynamics in tooth organogenesis. Sci. Signal. **5:**ra4. doi:10.1126/scisignal.2002414.
10. **Wang XP, Suomalainen M, Jorgez CJ, Matzuk MM, Werner S, Thesleff I.** 2004. Follistatin regulates enamel patterning in mouse incisors by asymmetrically inhibiting BMP signaling and ameloblast differentiation. Dev. Cell **7:**719–730.
11. **Diamond I, Owolabi T, Marco M, Lam C, Glick A.** 2000. Conditional gene expression in the epidermis of transgenic mice using the tetracycline-regulated transactivators tTA and rTA linked to the keratin 5 promoter. J. Investig. Dermatol. **115:**788–794.
12. **Perl AK, Wert SE, Nagy A, Lobe CG, Whitsett JA.** 2002. Early restriction of peripheral and proximal cell lineages during formation of the lung. Proc. Natl. Acad. Sci. U. S. A. **99:**10482–10487.
13. **Mishina Y, Hanks MC, Miura S, Tallquist MD, Behringer RR.** 2002. Generation of Bmpr/Alk3 conditional knockout mice. Genesis **32:**69–72.
14. **Huelsken J, Vogel R, Erdmann B, Cotsarelis G, Birchmeier W.** 2001. Beta-catenin controls hair follicle morphogenesis and stem cell differentiation in the skin. Cell **105:**533–545.
15. **Liu F, Chu EY, Watt B, Zhang Y, Gallant NM, Andl T, Yang SH, Lu MM, Piccolo S, Schmidt-Ullrich R, Taketo MM, Morrisey EE, Atit R, Dlugosz AA, Millar SE.** 2008. Wnt/beta-catenin signaling directs multiple stages of tooth morphogenesis. Dev. Biol. **313:**210–224.
16. **Han XL, Liu M, Voisey A, Ren YS, Kurimoto P, Gao T, Tefera L, Dechow P, Ke HZ, Feng JQ.** 2011. Post-natal effect of overexpressed DKK1 on mandibular molar formation. J. Dent. Res. **90:**1312–1317.
17. **Liu F, Dangaria S, Andl T, Zhang Y, Wright AC, Damek-Poprawa M, Piccolo S, Nagy A, Taketo MM, Diekwisch TG, Akintoye SO, Millar SE.** 2010. Beta-catenin initiates tooth neogenesis in adult rodent incisors. J. Dent. Res. **89:**909–914.
18. **Foster BL, Nagatomo KJ, Nociti FH, Jr, Fong H, Dunn D, Tran AB, Wang W, Narisawa S, Millan JL, Somerman MJ.** 2012. Central role of pyrophosphate in acellular cementum formation. PLoS One **7:**e38393. doi:10.1371/journal.pone.0038393.
19. **Hai B, Yang Z, Millar SE, Choi YS, Taketo MM, Nagy A, Liu F.** 2010. Wnt/beta-catenin signaling regulates postnatal development and regeneration of the salivary gland. Stem Cells Dev. **19:**1793–1801.
20. **Wang XP, Suomalainen M, Felszeghy S, Zelarayan LC, Alonso MT, Plikus MV, Maas RL, Chuong CM, Schimmang T, Thesleff I.** 2007. An integrated gene regulatory network controls stem cell proliferation in teeth. PLoS Biol. **5:**e159. doi:10.1371/journal.pbio.0050159.
21. **Hosoya A, Kim JY, Cho SW, Jung HS.** 2008. BMP4 signaling regulates formation of Hertwig's epithelial root sheath during tooth root development. Cell Tissue Res. **333:**503–509.
22. **Molla M, Descroix V, Aioub M, Simon S, Castaneda B, Hotton D, Bolanos A, Simon Y, Lezot F, Goubin G, Berdal A.** 2010. Enamel protein regulation and dental and periodontal physiopathology in MSX2 mutant mice. Am. J. Pathol. **177:**2516–2526.
23. **Sonoyama W, Seo BM, Yamaza T, Shi S.** 2007. Human Hertwig's epithelial root sheath cells play crucial roles in cementum formation. J. Dent. Res. **86:**594–599.
24. **Akimoto T, Fujiwara N, Kagiya T, Otsu K, Ishizeki K, Harada H.** 2011. Establishment of Hertwig's epithelial root sheath cell line from cells involved in epithelial-mesenchymal transition. Biochem. Biophys. Res. Commun. **404:**308–312.
25. **Thomas HF.** 1995. Root formation. Int. J. Dev. Biol. **39:**231–237.
26. **Obara N, Suzuki Y, Nagai Y, Takeda M.** 1999. Immunofluorescence detection of cadherins in mouse tooth germs during root development. Arch. Oral Biol. **44:**415–421.
27. **Zeichner-David M, Oishi K, Su Z, Zakartchenko V, Chen LS, Arzate H, Bringas P, Jr.** 2003. Role of Hertwig's epithelial root sheath cells in tooth root development. Dev. Dyn. **228:**651–663.
28. **Chang JY, Wang C, Jin C, Yang C, Huang Y, Liu J, McKeehan WL, D'Souza RN, Wang F.** 2013. Self-renewal and multilineage differentiation of mouse dental epithelial stem cells. Stem Cell Res. **11:**990–1002.
29. **Li L, Kwon HJ, Harada H, Ohshima H, Cho SW, Jung HS.** 2011. Expression patterns of ABCG2, Bmi-1, Oct-3/4, and Yap in the developing mouse incisor. Gene Expr. Patterns **11:**163–170.
30. **Nieto MA.** 2011. The ins and outs of the epithelial to mesenchymal transition in health and disease. Annu. Rev. Cell Dev. Biol. **27:**347–376.
31. **Woodcock SA, Rooney C, Liontos M, Connolly Y, Zoumpourlis V, Whetton AD, Gorgoulis VG, Malliri A.** 2009. SRC-induced disassembly of adherens junctions requires localized phosphorylation and degradation of the rac activator tiam1. Mol. Cell **33:**639–653.
32. **Samavarchi-Tehrani P, Golipour A, David L, Sung HK, Beyer TA, Datti A, Woltjen K, Nagy A, Wrana JL.** 2010. Functional genomics reveals a BMP-driven mesenchymal-to-epithelial transition in the initiation of somatic cell reprogramming. Cell Stem Cell **7:**64–77.
33. **Korpal M, Lee ES, Hu G, Kang Y.** 2008. The miR-200 family inhibits epithelial-mesenchymal transition and cancer cell migration by direct targeting of E-cadherin transcriptional repressors ZEB1 and ZEB2. J. Biol. Chem. **283:**14910–14914.
34. **Zeisberg M, Neilson EG.** 2009. Biomarkers for epithelial-mesenchymal transitions. J. Clin. Invest. **119:**1429–1437.
35. **Sugimoto H, Lebleu VS, Bosukonda D, Keck P, Taduri G, Bechtel W, Okada H, Carlson W, Bey P, Rusckowski M, Tampe B, Tampe D, Kanasaki K, Zeisberg M, Kalluri R.** 2012. Activin-like kinase 3 is impor-

tant for kidney regeneration and reversal of fibrosis. Nat. Med. **18:**396–404.
36. **Levy L, Hill CS.** 2005. Smad4 dependency defines two classes of transforming growth factor beta (TGF-beta) target genes and distinguishes TGF-beta-induced epithelial-mesenchymal transition from its antiproliferative and migratory responses. Mol. Cell. Biol. **25:**8108–8125.
37. **Heuberger J, Birchmeier W.** 2010. Interplay of cadherin-mediated cell adhesion and canonical Wnt signaling. Cold Spring Harb. Perspect. Biol. **2:**a002915. doi:10.1101/cshperspect.a002915.
38. **Xu B, Chen C, Chen H, Zheng SG, Bringas P, Jr, Xu M, Zhou X, Chen D, Umans L, Zwijsen A, Shi W.** 2011. Smad1 and its target gene Wif1 coordinate BMP and Wnt signaling activities to regulate fetal lung development. Development **138:**925–935.
39. **Kandyba E, Leung Y, Chen YB, Widelitz R, Chuong CM, Kobielak K.** 2013. Competitive balance of intrabulge BMP/Wnt signaling reveals a robust gene network ruling stem cell homeostasis and cyclic activation. Proc. Natl. Acad. Sci. U. S. A. **110:**1351–1356.
40. **Freeman TJ, Smith JJ, Chen X, Washington MK, Roland JT, Means AL, Eschrich SA, Yeatman TJ, Deane NG, Beauchamp RD.** 2012. Smad4-mediated signaling inhibits intestinal neoplasia by inhibiting expression of beta-catenin. Gastroenterology **142:**562–571.e2. doi:10.1053/j.gastro.2011.11.026.
41. **Xia H, Cheung WK, Sze J, Lu G, Jiang S, Yao H, Bian XW, Poon WS, Kung HF, Lin MC.** 2010. miR-200a regulates epithelial-mesenchymal to stem-like transition via ZEB2 and beta-catenin signaling. J. Biol. Chem. **285:**36995–37004.
42. **Tetsu O, McCormick F.** 1999. Beta-catenin regulates expression of cyclin D1 in colon carcinoma cells. Nature **398:**422–426.
43. **Willert J, Epping M, Pollack JR, Brown PO, Nusse R.** 2002. A transcriptional response to Wnt protein in human embryonic carcinoma cells. BMC Dev. Biol. **2:**8. doi:10.1186/1471-213X-2-8.
44. **Hirsinger E, Duprez D, Jouve C, Malapert P, Cooke J, Pourquie O.** 1997. Noggin acts downstream of Wnt and Sonic Hedgehog to antagonize BMP4 in avian somite patterning. Development **124:**4605–4614.
45. **Malanchi I, Santamaria-Martinez A, Susanto E, Peng H, Lehr HA, Delaloye JF, Huelsken J.** 2012. Interactions between cancer stem cells and their niche govern metastatic colonization. Nature **481:**85–89.
46. **Liu Z, Tang Y, Qiu T, Cao X, Clemens TL.** 2006. A dishevelled-1/Smad1 interaction couples WNT and bone morphogenetic protein signaling pathways in uncommitted bone marrow stromal cells. J. Biol. Chem. **281:**17156–17163.
47. **Dong J, Amor D, Aldred MJ, Gu T, Escamilla M, MacDougall M.** 2005. DLX3 mutation associated with autosomal dominant amelogenesis imperfecta with taurodontism. Am. J. Med. Genet. A **133A:**138–141.
48. **Hwang J, Mehrani T, Millar SE, Morasso MI.** 2008. Dlx3 is a crucial regulator of hair follicle differentiation and cycling. Development **135:**3149–3159.
49. **Zhai Y, Iura A, Yeasmin S, Wiese AB, Wu R, Feng Y, Fearon ER, Cho KR.** 2011. MSX2 is an oncogenic downstream target of activated WNT signaling in ovarian endometrioid adenocarcinoma. Oncogene **30:**4152–4162.
50. **Laurikkala J, Kassai Y, Pakkasjarvi L, Thesleff I, Itoh N.** 2003. Identification of a secreted BMP antagonist, ectodin, integrating BMP, FGF, and SHH signals from the tooth enamel knot. Dev. Biol. **264:**91–105.
51. **Yokohama-Tamaki T, Ohshima H, Fujiwara N, Takada Y, Ichimori Y, Wakisaka S, Ohuchi H, Harada H.** 2006. Cessation of Fgf10 signaling, resulting in a defective dental epithelial stem cell compartment, leads to the transition from crown to root formation. Development **133:**1359–1366.
52. **Hu X, Wang Y, He F, Li L, Zheng Y, Zhang Y, Chen YP.** 2012. Noggin is required for early development of murine upper incisors. J. Dent. Res. **91:**394–400.
53. **Sakano M, Otsu K, Fujiwara N, Fukumoto S, Yamada A, Harada H.** 2013. Cell dynamics in cervical loop epithelium during transition from crown to root: implications for Hertwig's epithelial root sheath formation. J. Periodontal Res. **48:**262–267.
54. **Wang XP, Suomalainen M, Jorgez CJ, Matzuk MM, Wankell M, Werner S, Thesleff I.** 2004. Modulation of activin/bone morphogenetic protein signaling by follistatin is required for the morphogenesis of mouse molar teeth. Dev. Dyn. **231:**98–108.
55. **Lohi M, Tucker AS, Sharpe PT.** 2010. Expression of Axin2 indicates a role for canonical Wnt signaling in development of the crown and root during pre- and postnatal tooth development. Dev. Dyn. **239:**160–167.
56. **Yamashiro T, Zheng L, Shitaku Y, Saito M, Tsubakimoto T, Takada K, Takano-Yamamoto T, Thesleff I.** 2007. Wnt10a regulates dentin sialophosphoprotein mRNA expression and possibly links odontoblast differentiation and tooth morphogenesis. Differentiation **75:**452–462.
57. **Yan C, Grimm WA, Garner WL, Qin L, Travis T, Tan N, Han YP.** 2010. Epithelial to mesenchymal transition in human skin wound healing is induced by tumor necrosis factor-alpha through bone morphogenic protein-2. Am. J. Pathol. **176:**2247–2258.
58. **Ma L, Lu MF, Schwartz RJ, Martin JF.** 2005. Bmp2 is essential for cardiac cushion epithelial-mesenchymal transition and myocardial patterning. Development **132:**5601–5611.
59. **Zeisberg M, Hanai J, Sugimoto H, Mammoto T, Charytan D, Strutz F, Kalluri R.** 2003. BMP-7 counteracts TGF-beta1-induced epithelial-to-mesenchymal transition and reverses chronic renal injury. Nat. Med. **9:**964–968.
60. **Li J, Huang X, Xu X, Mayo J, Bringas P, Jr, Jiang R, Wang S, Chai Y.** 2011. SMAD4-mediated WNT signaling controls the fate of cranial neural crest cells during tooth morphogenesis. Development **138:**1977–1989.